

# Analytic Formulas for the Orientation Dependence of Step Stiffness and Line Tension: Key Ingredients for Numerical Modeling

T. J. Stasevich\* and T. L. Einstein†

*Department of Physics, University of Maryland, College Park, MD 20742-4111*

(Dated: June 12, 2006)

We present explicit analytic, twice-differentiable expressions for the temperature-dependent anisotropic step line tension and step stiffness for the two principal surfaces of face-centered-cubic crystals, the square  $\{001\}$  and the hexagonal  $\{111\}$ . These expressions improve on simple expressions that are valid only for low temperatures and away from singular orientations. They are well suited for implementation into numerical methods such as finite-element simulation of step evolution.

AMS codes: 82B24, 80M10, 35Q99, 82C05, 76M28

Keywords: step stiffness, step line tension, anisotropy, numerical modeling, finite-element simulation, step dynamics

## INTRODUCTION

Numerical study of the shape and evolution of layered island structures on surfaces has become an active field [1, 2, 3, 4, 5]. These investigations typically focus on the motion of the island boundaries, which amount to variously oriented single-layer-high steps. A crucial ingredient then is the step line tension (free energy per length)  $\beta(\theta)$ , where  $\theta$  gives the step orientation (the angle of its in-plane normal with respect to a reference high-symmetry direction), or the step stiffness  $\tilde{\beta}(\theta) \equiv \beta(\theta) + \beta''(\theta)$ , which serves as the inertial parameter in the Schrödinger equation when steps are represented by evolving fermions [6] and is one of the three parameters of the step-continuum model [7]. Practically speaking, the line tension controls the equilibrium shapes of single-layer island structures, while the stiffness controls the fluctuations about those equilibrium shapes.

If one assumes that step adatoms interact with only nearest-neighbors (NN) or next-nearest-neighbors (NNN), then it is possible to derive exact solutions for the line tension based on the Ising or solid-on-solid (SOS) models. These solutions are implicit, however, making their implementation into numerical simulations time-consuming and computationally demanding, particularly when dealing with the stiffness, which requires two additional derivatives of the implicit line tension. For simplicity, then, numerical studies often [2, 3] (though by no means always [4]) assume an isotropic line tension and stiffness. Except at high temperatures where an island structure is nearly circular, this approximation turns out to be poor, especially near facet orientations. The next simplest approximation assumes a sinusoidal variation reflecting the substrate symmetry [5]. Again, there are shortcomings to this procedure, especially near facet orientations. Such temperature-independent simplifications allow for only qualitative comparisons with experiment.

In this paper we construct expressions for  $\beta(\theta)$  and  $\tilde{\beta}(\theta)$  that are well behaved analytically, being continu-

ous and twice differentiable, and that give an accurate accounting at all orientations and relevant temperatures. While not especially simple, they are straightforward to construct and easy to implement in numerical codes such as used in finite-element investigations [8, 9], making quantitative comparisons with dynamic experiments possible. We thus expect our results to be widely applicable.

Our approach begins with simple, low-temperature formulas for the orientation dependence, on face-centered-cubic (fcc) surfaces, of the  $\{001\}$  and  $\{111\}$  stiffness and line tension that we derived in two recent papers [11, 12]. (This approach is rooted in the lattice-gas perspective, so is complementary to Shenoy and Ciobanu's study of stiffness anisotropy based on elasticity theory [13].) Our formulas assume the step fluctuations are dominated by the rearrangement of geometrically forced kinks—kinks that are not thermally activated. At temperatures low compared to the surface roughening temperature (for noble metal surfaces, such as Ag and Cu, room temperature is considered “low”), the formulas only fail for steps having a negligible number of forced kinks; that is, steps oriented very close to the high-symmetry direction. When the step angle is exactly  $0^\circ$  (aligned with the high-symmetry direction), the formulas predict a cusp in the line-tension and an infinite step stiffness. Here we correct for the non-analytic behavior by splicing our simple, low-temperature formulas with small-angle expansions of the exact, implicit solutions based on the Ising and SOS models.

In the following section, we describe the details of a general expansion for the stiffness and line tension that is continuous and twice-differentiable. In sections III and IV, we apply this expansion to fcc  $\{111\}$  and  $\{001\}$  surfaces, respectively, to derive surface-specific formulas for the stiffness and line tension. In the final section, we offer concluding remarks as well as a synopsis of the derived expressions.

## EXPLICIT ANALYTIC APPROXIMATION

At the microscopic level, the step stiffness and line tension arise from the energy and rearrangement of step edge kinks. It is therefore natural to decompose  $\tilde{\beta}(\theta)$  and  $\beta(\theta)$  into two contributions: one part originating from geometrically forced kinks and one part from thermally activated kinks. Geometrically forced kinks, depicted in the inset of Fig. 1, are present at all temperatures, and give the step an overall orientation  $\theta$ . The further  $\theta$  is from the high symmetry direction, the greater the number of geometrically forced kinks. Thus, at lower temperatures, as long as the orientation angle of a step is *greater* than some small, temperature-dependent cross-over angle  $\theta_c$ , there are many geometrically forced kinks and relatively few thermally activated kinks, suggesting  $\tilde{\beta}(\theta)$  and  $\beta(\theta)$  can be well described by formulas based on geometrically forced kinks alone.

As an example, we have recently derived [11] a remarkably simple, low-temperature formula for the  $\{111\}$  step stiffness assuming only NN adatom interactions and geometrically forced kinks:

$$\frac{k_B T}{\tilde{\beta}(\theta)} \approx \frac{\sin(3\theta)}{2\sqrt{3}}. \quad (1)$$

At sufficiently low (but experimentally relevant) temperatures, the formula works well for steps at nearly all angles, but predicts an infinite stiffness when  $\theta = 0$ . Fortunately, the exact, implicit solution based on the NN Ising model can be explicitly written for steps having this orientation. We can therefore expand the exact solution about  $\theta = 0$  and splice it with our low-temperature solution at  $\theta_c$ , thereby producing an explicit form for  $\tilde{\beta}(\theta)$  valid at all angles. This idea is illustrated in Fig. (1). Here, an additional orientation-dependent contribution to the stiffness from thermally activated kinks  $\Delta$  is also included for completeness. Similar to high-symmetry steps, the stiffness of maximally kinked steps ( $\theta = \pi/6$ ) can be exactly obtained from the NN Ising model, so that  $\Delta$  can be determined explicitly.

To generalize this approach, we assume  $\tilde{\beta}(\theta)$  and  $\beta(\theta)$  are well described at angles *greater* than  $\theta_c$  by simple, analytic functions representing contributions from geometrically forced kinks. Explicit forms for these functions [11, 12] will be discussed later. For now, to be general, we simply write them as  $f(\theta)$ .

At sufficiently low temperatures,  $\theta_c$  is small, so we may accurately represent  $\beta(\theta)$  and the inverse stiffness  $\tilde{\beta}^{-1}(\theta)$  at angles *less* than  $\theta_c$  using small-angle expansions. (We expand the inverse stiffness because, in the  $\theta=0$  limit, it vanishes at low temperatures, making it mathematically better behaved than the stiffness itself, which diverges). Specifically, we construct an approximant  $X(\theta)$  to represent the dimensionless form of the function we wish to expand—either  $\beta(\theta)a_{||}/(k_B T)$  or  $k_B T/(\tilde{\beta}(\theta)a_{||})$ , where

$a_{||}$  is the close-packed distance between atoms (i.e. the atomic diameter), and  $k_B T$  is the Boltzmann energy—we define

$$X(\theta) := \begin{cases} \sum_{n=0}^{2N-1} a_n \theta^n & \text{if } \theta < \theta_c, \\ f(\theta) & \text{if } \theta \geq \theta_c \end{cases}, \quad (2)$$

where  $n$  is a non-negative integer between zero and an odd integer  $2N - 1$ . To fully specify this function, we must find the appropriate expansion coefficients,  $a_n$ . We obtain their values by matching Eq. (2) and its higher order derivatives with the exact solutions at  $\theta=0$  (which can be systematically obtained) and the approximate (yet accurate) solutions obtained from  $f(\theta)$  at  $\theta = \theta_c$ , analogous to performing a spline fit [15]. Specifically, for the boundary conditions at  $\theta = 0$ , we have

$$a_n = \frac{\partial_\theta^n X(0)}{n!}, \quad n < N \quad (3)$$

where  $\partial_\theta^n X(0) \equiv \partial^n X(\theta)/\partial\theta^n|_{\theta=0}$ . The remaining  $N$  coefficients are found from the boundary conditions at  $\theta = \theta_c$ , which form a set of  $N$  coupled linear equations:

$$\sum_{n=N}^{2N-1} \frac{n!}{(n-m)!} a_n \theta_c^{n-m} = \partial_\theta^m f(\theta_c), \quad (4)$$

where  $m$  is a non-negative integer less than  $N$ .

For use in continuum models,  $\tilde{\beta}(\theta)$  should be continuous and twice-differentiable. To ensure the second derivative remains continuous at  $\theta = \theta_c$ , this requires, at minimum,  $N = 3$ . In this case, Eqs. (4) are simultaneously solved to give:

$$a_3 = \frac{20(f - X) - 8f' \theta_c + (f'' - 3X'') \theta_c^2}{2 \theta_c^3} \quad (5)$$

$$a_4 = \frac{-30(f - X) + 14f' \theta_c - (2f'' - 3X'') \theta_c^2}{2 \theta_c^4} \quad (6)$$

$$a_5 = \frac{12(f - X) - 6f' \theta_c + (f'' - X'') \theta_c^2}{2 \theta_c^5}, \quad (7)$$

where the prime represents differentiation with respect to  $\theta$ ; for brevity we write  $f \equiv f(\theta_c)$  and  $X \equiv X(0)$ . Note we have also used Eq. (3), which implies  $a_0 = X$ ,  $a_1 = X'$ , and  $a_2 = X''/2$ . Because both the line tension and the stiffness are continuous and symmetric about  $\theta=0$ , we know that  $a_1 = X' = 0$ . In the remaining sections we apply this approximation to specific cases where explicit forms for  $X$  and  $f$  can be obtained.

## $\{111\}$ SURFACES WITH NN INTERACTIONS

For  $\{111\}$  surfaces with only NN adatom interactions, Zia found an implicit form for the full orientation dependence of the step line tension [14]:

$$\frac{\beta a_{||}}{k_B T} = \eta_0(\theta)\psi_1(\theta, T/T_c) + \eta_-(\theta)\psi_2(\theta, T/T_c), \quad (8)$$

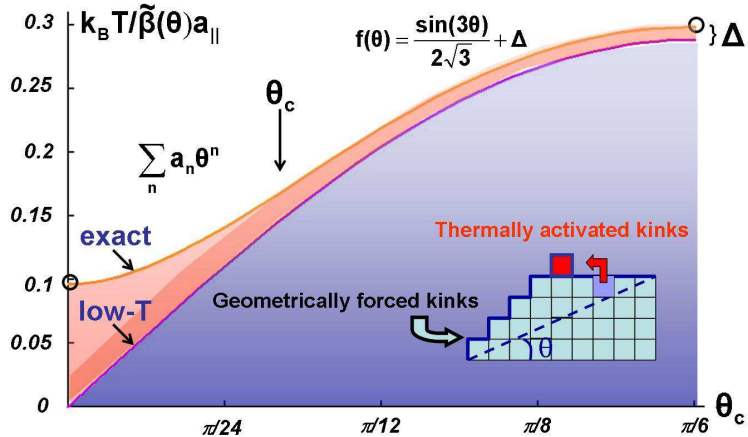


FIG. 1: The contributions to the step stiffness can be decomposed into parts originating from geometrically forced kinks (lower blue region bounded from above by the line labeled “low-T”) and thermally activated kinks (the remaining red region, bounded from above by the line labeled “exact”). At relatively low-temperatures, the {111} step stiffness is well approximated at angles greater than  $\theta_c$  by a relatively simple, explicit function  $f(\theta)$ , since the thermal part is evidently insensitive to angle. To account for all angles, the formula can be spliced with a small-angle expansion of the exact NN Ising model solution (from which explicit forms for the stiffness can be obtained at  $\theta = 0$  and at  $\pi/6$ , depicted here by hollow circles). The solution at  $\pi/6$  is used to determine  $\Delta$ . The expansion coefficients  $a_n$  are obtained by matching the solutions at  $\theta = 0$  and  $\theta_c$ . The inset depicts a step edge from above. Each square represents an adatom which is part of the step edge. The upper-most square represents a thermally excited adatom, which forms four thermally-activated kinks. The remaining kinks are geometrically forced—they must be present to give the step edge an overall angle  $\theta$ .

where  $\eta_0(\theta) \equiv (2/\sqrt{3}) \sin(\theta)$ ,  $\eta_{\pm}(\theta) \equiv \cos(\theta) \pm (1/\sqrt{3}) \sin(\theta)$ . Here  $T_c$  is the critical temperature of the NN lattice-gas model. The  $\psi$ ’s are solutions of the pair of simultaneous equations for the angular constraint,

$$\frac{\sinh(\psi_1 - \frac{1}{2}\psi_2) \cosh(\frac{1}{2}\psi_2)}{\sinh(\psi_2 - \frac{1}{2}\psi_1) \cosh(\frac{1}{2}\psi_1)} = \frac{\eta_0}{\eta_{\pm}}, \quad (9)$$

and the thermal constraint,

$$\cosh \psi_1 + \cosh \psi_2 + \cosh(\psi_1 - \psi_2) = \frac{y^2 - 3}{2}, \quad (10)$$

where  $y \equiv \sqrt{(3z + 1)/z(1 - z)}$  and  $z \equiv 3^{-T_c/T}$ . The latter can be rewritten  $z \equiv \exp(-2\epsilon_k/k_B T)$ , where  $\epsilon_k$  is the energy of a kink on a close-packed step and

$$\frac{\epsilon_k}{k_B T_c} = \ln \sqrt{3} \quad (11)$$

From Eqs. (9,10) it follows that

$$\psi_1(0) = \frac{1}{2}\psi_2(0) = \cosh^{-1} \left( \frac{y - 1}{2} \right). \quad (12)$$

With  $\psi_1(0)$  and  $\psi_2(0)$  in hand, we can differentiate the constraints, Eqs. (9,10), set  $\theta = 0$ , and systematically solve for all the higher order derivatives of the  $\psi$ ’s, which, according to Eq. (8), are sufficient to find the higher order derivatives of  $\beta$ . We will utilize these higher order derivatives to derive explicit, analytic approximations for the stiffness and line tension.

### Step Stiffness

In this case,  $X(\theta) \equiv k_B T / (\tilde{\beta}(\theta) a_{||})$ , which is six-fold symmetric for {111} surfaces with only NN adatom interactions. To utilize our explicit analytic approximation, we require  $f(\theta)$ —the contribution to the reduced stiffness from geometrically forced kinks—which, in the first sextant ( $-\pi/6$  to  $\pi/6$ ), takes a relatively simple form [12]:

$$f(\theta) = \frac{1}{2\sqrt{3}} \left( \sin(3\theta) + \frac{3 + y^2}{\sqrt{y^4 - 10y^2 + 9}} - 1 \right). \quad (13)$$

The last two terms, called  $\Delta$  in Fig. 1, are included to ensure  $f(\theta)$  matches the exact solution for steps with orientation angle  $\theta = \pi/6$ . The physical origin of the  $\Delta$  terms is the thermal fluctuations of a maximally kinked step. Such fluctuations are relatively inexpensive in terms of energy. They dominate the fluctuation contribution while a significant fraction of the step is not close-packed, so that the thermal contribution for such orientations is relatively independent of orientation. Since only the first term has any  $\theta$  dependence,  $f'$  and  $f''$  are simple to calculate.

Now only  $X$  and its first two derivatives need to be determined. As mentioned in the preceding section, these can be systematically determined. In particular, we find (see Eq. (23) for a derivation of  $X$  in our earlier paper

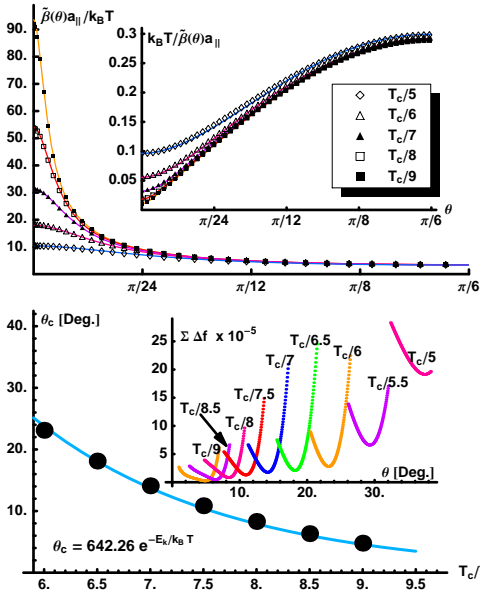


FIG. 2: In the left plot, the orientation dependence of our explicit approximation for the  $\{111\}$  step stiffness (solid lines) and its inverse (inset, solid lines) are compared to the exact, implicit solutions (shapes). Because of the six-fold symmetry of the solution, only the positive half of the first sextant is shown (the negative half is mirror-symmetric). The right plot shows the values used for  $\theta_c$  (solid dots) in the construction of the left figure and the corresponding exponential fit (solid line), good over the temperature range of interest. The fit is expressed in terms of the kink energy  $\epsilon_k$ , which is related to  $T_c$  by Eq. (11). The inset shows the sum of errors ( $\sum \Delta f^2$ ) versus angle in the least square fit for  $\theta_c$ . At each temperature,  $\theta_c$  is the angle that minimizes this sum.

[12]):

$$X \equiv \frac{k_B T}{a_{||} \tilde{\beta}(0)} = \frac{3(y-1)}{2y\sqrt{y^2-2y-3}}, \quad (14)$$

$$X' = 0, \quad (15)$$

$$X'' = \frac{y^3 - 2y^2 - 15y + 36}{2(y-1)\sqrt{y^2-2y-3}}. \quad (16)$$

Of course, based on symmetry, we already knew that  $X' = 0$ .

By combining the functional forms for  $f$  and  $X$  and their derivatives with Eqs. (2-7), we can plot the stiffness and compare it to the numerically evaluated exact solution. We show this comparison in Fig. 2, where  $\theta_c$  was determined at a variety of temperatures by doing least square fits to the exact solution. The agreement shown in Fig. 2 is very good at low-temperatures and is quite reasonable at temperatures all the way up to  $T_c/5$ . (This behavior is remarkable since slightly above  $T_c/5.5$ ,  $\theta_c$  becomes greater than  $30^\circ$ , i.e., the power series is used for the entire range of orientations. Once  $|\theta_c| > 30^\circ$ , the slope of  $k_B T / a_{||} \tilde{\beta}(\theta)$  no longer vanishes

at  $30^\circ$ .) At higher temperatures, the angular dependence becomes negligible, so  $\tilde{\beta}(\theta)$  become isotropic.

The right plot in Fig. 2 shows the values used for  $\theta_c$ , along with an exponential fit:

$$\theta_c(T) \approx 642.26(\sqrt{3})^{-T_c/T} = 642.26 \exp(-\epsilon_k/k_B T). \quad (17)$$

The Arrhenius decay reflects the importance of thermally-activated kinks for  $|\theta| < \theta_c$ .

### Step Line Tension

We follow the same procedure for the line tension. In this case  $X(\theta) \equiv \beta(\theta) a_{||} / k_B T$ . The contribution (in the first sextant) to the line tension from geometrically forced kinks is also fairly simple [11]:

$$f(\theta) = -\eta_+ \ln z - \eta_+ \ln \eta_+ + \eta_- \ln \eta_- + \eta_0 \ln \eta_0. \quad (18)$$

Just as for the stiffness, we systematically determine  $X$  and its first two derivatives by differentiating the exact solution, Eqs. (8-12),

$$X \equiv \frac{a_{||} \beta(0)}{k_B T} = 2 \cosh^{-1} \left( \frac{y-1}{2} \right), \quad (19)$$

$$X' = 0, \quad (20)$$

$$X'' = \frac{2y\sqrt{y^2-2y-3}}{3(y-1)} - X. \quad (21)$$

The last equation can be rearranged to find the reduced stiffness at  $\theta = 0$ , as expressed earlier in Eq. (14). With these parameters in hand, we compare our approximation for the full orientation dependence of the reduced line tension with the exact, numerically evaluated solution in

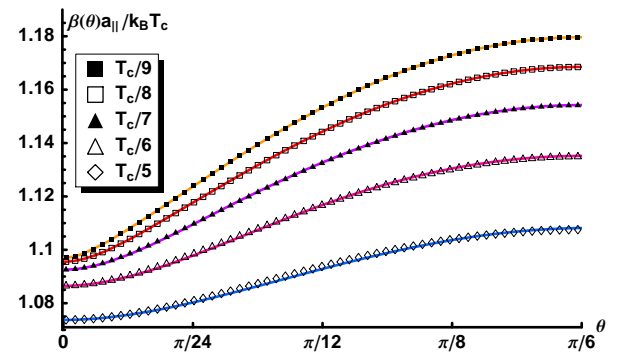


FIG. 3: The orientation dependence of the explicit approximation for the  $\{111\}$  line tension (solid lines) is compared with the numerically evaluated exact result (shapes). Because of the six-fold symmetry, only the positive half of the first sextant is shown. (The negative half is mirror symmetric.)

Fig. 3. For the critical angle, we use Eq. (17). As before, the fit works remarkably well at temperatures as high as  $T_c/5$ .

### {001} SURFACES WITH NN AND NNN INTERACTIONS

#### Step Stiffness

To begin, we let  $X(\theta) \equiv k_B T / (\tilde{\beta}(\theta) a_{||})$ . The symmetry of {001} surfaces require  $X(\theta)$  be four-fold symmetric. Accounting for just geometrically forced kinks, the reduced inverse stiffness is well approximated in the first quadrant ( $-\pi/4$  to  $\pi/4$ ) for  $|\theta| > \theta_c$  by the following function [11]:

$$f(\theta) = \frac{\sin(2\theta)}{2} \sqrt{1 - y \sin(2\theta)}. \quad (22)$$

By differentiating Eq. (22),  $f'$  and  $f''$  are easily obtained.

To determine  $X$ ,  $X'$ , and  $X''$  (and, potentially, any higher order derivatives), we utilize the exact solution of the NNN SOS model. Eq. (28), for example, implies that  $\rho_0 = 0$  when  $\theta = 0$ . With some effort, it can be shown that

$$X = \frac{2 \sinh S}{(\cosh S - 1)[2 \sinh S - (\cosh S - 1)(y + 1)]} \quad (23)$$

$$X' = 0 \quad (24)$$

$$X'' = \frac{1}{X} \frac{2 \cosh S + 1}{\cosh S - 1} - 4 \left[ \frac{\cosh S - 1}{\sinh S} \frac{y + 1}{2} + X \right]. \quad (25)$$

As required by symmetry,  $X' = 0$ .

Combining the functional forms for  $f$ ,  $X$ , and their derivatives with Eqs. (2-7), we can plot the inverse step stiffness and compare it to the numerically evaluated exact solution, just as before. We show this comparison in Fig. 4, where  $\theta_c$  was determined by doing least square fits to the numerically evaluated exact solution (with  $R = 1/5$ ). The agreement shown in Fig. 4 is excellent at low-temperatures and is very reasonable at temperatures all the way up to  $T_c/5$ , as was the case for the {111} solution.

Although it was not initially obvious, the relative size of the NNN interaction  $R$  has little effect on  $\theta_c$ . This fortuitously implies that a single  $\theta_c$  works for all values of  $R$ , as depicted in the lower plots of Fig. 4.

With this in mind, the values used for  $\theta_c$  were determined just as they were for the {111} case, but with  $R = 1/5$ . These are shown in the upper-right plot of Fig. 4, as well as a simple fit that is accurate over the temperature range of interest:

$$\theta_c(T) \approx 384.86 e^{-\epsilon_k/k_B T} = 384.86(1 + \sqrt{2})^{-T_c/T}. \quad (26)$$

Again, the Arrhenius decay is anticipated since  $\theta_c$  represents the angle below which thermally activated kinks on close-packed segments become important.

For {001} surfaces with just NN interactions, an exact, explicit form for the full orientation dependence of the line tension was first determined by Abraham and Reed [16]. For such surfaces, however, NNN interactions are often significant [11], so it is desirable to find a solution including their effects. We denote by  $R$  the ratio of NNN to NN adatom interaction strengths; the latter is assumed to be attractive (negative), so a positive  $R$  indicates that the NNN interaction also is.

Although no exact solution to the Ising model with both NN and NNN interactions exists, the solid-on-solid (SOS) model provides an excellent approximation at reasonable temperatures ( $\sim T_c/2$  based on our comparisons with the imaginary path weight random-walk method developed by the Akutsus [17]). This model can be solved exactly [11], yielding the following implicit form for the reduced line-tension:

$$\frac{\beta(\theta) a_{||}}{k_B T} = \rho(\theta) \sin \theta + g(\rho(\theta)), \quad (27)$$

where  $\rho(\theta)$  is found by inverting

$$\tan \theta = \frac{2 \sinh \rho \sinh S}{(\cosh S - \cosh \rho)[2 \sinh S - (\cosh S - \cosh \rho)(y + 1)]}, \quad (28)$$

while  $g(\rho)$  is

$$g(\rho) = S - \ln \left( \frac{y + 1}{y - 1} + \frac{2}{1 - y} \frac{\sinh S}{\cosh S - \cosh \rho} \right). \quad (29)$$

Here  $y \equiv 1 - 2z^R$ ,  $S \equiv -(R + 1/2) \ln z$ ,  $z \equiv (1 + \sqrt{2})^{-2T_c/T} = \exp(-\epsilon_k/k_B T)$ , while  $T_c$  is the critical temperature for  $R = 0$  (just NN interactions):

$$\frac{\epsilon_k}{k_B T_c} = \ln(1 + \sqrt{2}), \quad (30)$$

where the kink energy  $\epsilon_k$  now refers to a close-packed step on an {001} surface. We will utilize the exact, implicit solution Eqs. (27-29) to determine the parameters required to find an explicit approximation for the stiffness and line tension below.

Finally, we point out that the {001} step stiffness is much more anisotropic than its {111} counterpart. In fact, at  $T_c/6$  the anisotropy is as large as the {111} anisotropy at  $T_c/9$ . Furthermore,  $\theta_c$  is less sensitive to temperature than its {111} counterpart. This follows from the relative ease of thermally activating kinks on {111} steps, requiring only the breaking of one NN bond, as compared to two for {001} steps. For {111} steps, then, the angle  $\theta_c$  below which thermally activated kinks become important is larger than for {001} steps.

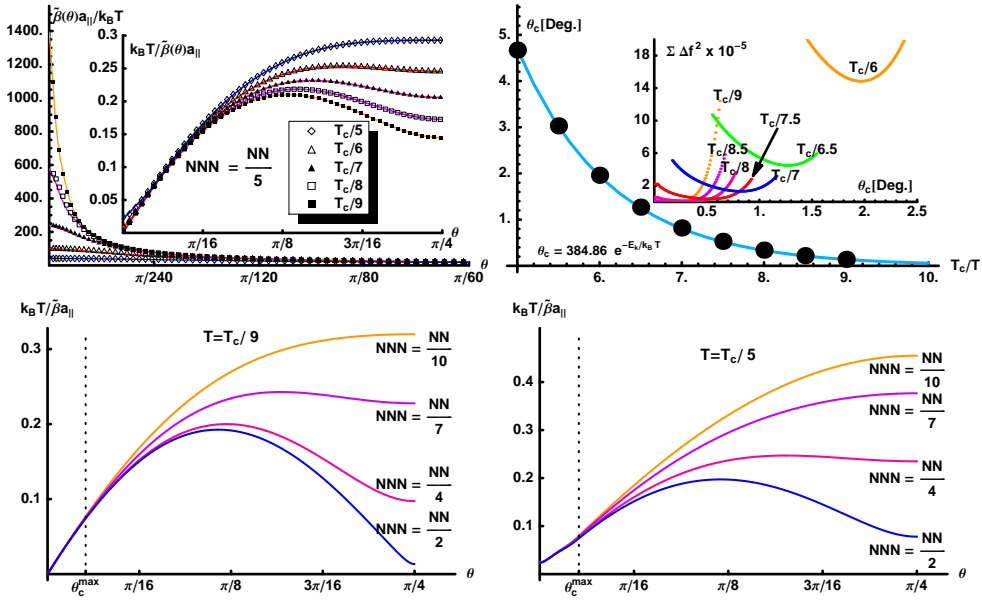


FIG. 4: In the upper-left plot the orientation dependence of the explicit approximation for the  $\{001\}$  step stiffness (solid lines) and its inverse (inset, solid lines) are compared to the exact, implicit solutions (shapes). Because of the four-fold symmetry of the solution, only the positive half of the first quadrant is shown (the negative half is mirror-symmetric). The upper-right plot shows the values used for  $\theta_c$  (solid dots) in the construction of the upper-left figure and the corresponding exponential decay fit (solid line) good over the temperature range of interest. The fit is expressed in terms of the kink energy  $\epsilon_k$  which is related to  $T_c$  by Eq. (30). The inset shows the sum of errors ( $\sum \Delta f^2$ ) versus angle in the least square fit for  $\theta_c$ . At each temperature,  $\theta_c$  is the angle that minimizes the sum of error. The two lower plots show the  $\{001\}$  inverse stiffness for a variety of different  $R$  at two temperatures,  $T_c/9$  and  $T_c/5$  (the extremum of the temperature range of interest). Notice that for a given temperature, all curves align at an angle greater than the largest critical angle  $\theta_c^{\max}$ . This behavior means  $\theta_c$ , practically speaking, does not depend on  $R$  at these temperatures.

### Step Line Tension

We proceed as usual, letting  $X(\theta) \equiv \beta(\theta)a_{||}/k_B T$ . The contribution from geometrically forced kinks is found by solving the low-temperature form of Eq. (28), which becomes quadratic in  $e^{\rho-S}$ . Solving gives

$$e^{\rho-S} = \frac{\sqrt{1 - y \sin(2\theta)} + y \sin \theta - \cos \theta}{(1 + y) \sin \theta}. \quad (31)$$

Plugging this into Eq. (27) yields an excellent approximation  $f(\theta)$  for the reduced line tension  $X(\theta)$  valid in the first quadrant ( $-\pi/4$  to  $\pi/4$ ) for  $|\theta| > \theta_c$ :

$$f(\theta) = \cos \theta \left[ S + \ln \frac{(1-y)(\sin \theta + \cos \theta - \sqrt{1-y \sin(2\theta)})}{(1+y)(\sin \theta - \cos \theta + y \sqrt{1-y \sin(2\theta)})} \right] + \sin \theta \left[ S + \ln \frac{\sqrt{1-y \sin(2\theta)} + y \sin \theta - \cos \theta}{(1+y) \sin \theta} \right] \quad (32)$$

Differentiating twice straightforwardly gives  $f'$  and  $f''$ . Eq. (32) can be written more compactly by defining and inserting  $w(\theta, y) \equiv [\cos \theta - \sqrt{1-y \sin(2\theta)}] / \sin \theta$ , as done in Table I.

This leaves  $X$  and its derivatives. They too can be explicitly determined from the exact solution. Setting both  $\theta = 0$  and  $\rho = 0$  (as Eq. (28) demands) in Eq. (27),

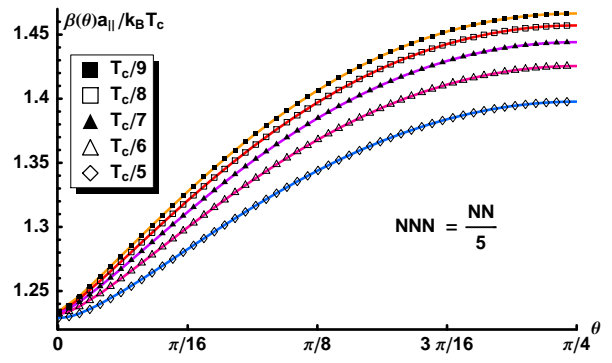


FIG. 5: The orientation dependence of the explicit approximation for the  $\{001\}$  line tension (solid lines) is compared with the numerically evaluated exact result (shapes). Because of the four-fold symmetry, only the positive half of the first quadrant is shown (the negative half is mirror symmetric).

EXPLICIT APPROXIMATION FOR STIFFNESS AND LINE TENSION					
$X(\theta) := \begin{cases} \sum_{n=0}^{2N-1} a_n \theta^n, & \theta < \theta_c \\ f(\theta), & \theta \geq \theta_c \end{cases}$ $a_0 = X \quad a_3 = \frac{20(f-X)-8f' \theta_c+(f''-3X'') \theta_c^2}{2 \theta_c^3}$ $a_1 = 0 \quad a_4 = \frac{-30(f-X)+14f' \theta_c-(2f''-3X'') \theta_c^2}{2 \theta_c^4}$ $a_2 = \frac{X''}{2} \quad a_5 = \frac{12(f-X)-6f' \theta_c+(f''-X'') \theta_c^2}{2 \theta_c^5}$					
{111} Surfaces with NN Interactions					
↓	$\theta_c = 642.26 e^{-\epsilon_k/k_B T}, \quad z = 3^{-T_c/T} = e^{-2\epsilon_k/k_B T}, \quad y = \sqrt{(3z+1)/z(1-z)}$				
	<b>Stiffness</b> ( $X(\theta) \approx k_B T/a_{  }\tilde{\beta}$ ) <b>Line Tension</b> ( $X(\theta) \approx a_{  }\beta/k_B T$ )				
$X$	$\frac{3(y-1)}{2y\sqrt{y^2-2y-3}}$				
$X''$	$\frac{y^3-2y^2-15y+36}{2(y-1)\sqrt{y^2-2y-3}}$				
$f(\theta)$	$\frac{1}{2\sqrt{3}} \left( \sin(3\theta) + \frac{3+y^2}{\sqrt{y^4-10y^2+9}} - 1 \right)$				
$X$	$\frac{2 \sinh S}{(\cosh S-1)[2 \sinh S-(\cosh S-1)(y+1)]}$				
$X''$	$\frac{1}{X} \frac{2 \cosh S+1}{\cosh S-1} - 4 \left[ \frac{\cosh S-1}{\sinh S} \frac{y+1}{2} + X \right]$				
$f(\theta)$	$\frac{\sin(2\theta)}{2} \sqrt{1-y \sin(2\theta)}$				
{001} Surfaces with NN and NNN (= $\mathbf{R} \times \mathbf{N}$ ) Interactions					
↑	$\theta_c = 384.86 e^{-\epsilon_k/k_B T}, \quad z = e^{-2\epsilon_k/k_B T} = (1+\sqrt{2})^{-2T_c/T}, \quad S = (1+2R) \epsilon_k/k_B T, \quad y = 1-2z^R$				
* $\eta_{\pm} \equiv \cos \theta \pm \frac{1}{\sqrt{3}} \sin \theta, \quad \eta_0 \equiv \frac{2}{\sqrt{3}} \sin \theta$			† $w(\theta, y) \equiv \cot \theta - \csc \theta \sqrt{1-y \sin(2\theta)}$		

TABLE I: Summary of results for approximants of dimensionless inverse stiffness and line tension.  $X \equiv X(0)$ , while  $f \equiv f(\theta_c)$ . The upper part of the table (dark red) refers to the steps on the hexagonal-lattice face, with just NN interactions. The lower part (blue) refers to the square-lattice face; by setting  $R=0$ , one retrieves the simpler formulas for just NN interactions.

we find  $X$ :

$$\begin{aligned} X &= g(0) \\ &= S - \ln \left( \frac{y+1}{y-1} + \frac{2}{1-y} \frac{\sinh S}{\cosh S - 1} \right). \end{aligned} \quad (33)$$

Similarly, it can be shown that

$$X' = 0, \quad (34)$$

$$X'' = \frac{(\cosh S-1)[2 \sinh S-(\cosh S-1)(y+1)]}{2 \sinh S} - X. \quad (35)$$

This last equation can be rearranged to give the reduced step stiffness, as previously written in Eq. (23).

By combining the functional forms for  $f$  and  $X$  and their derivatives with Eqs. (2-7), we can plot the reduced line tension and compare it to the numerically evaluated exact solution. We show this comparison in Fig. 5, where  $\theta_c$  was determined from Eq. (26) and  $R = 1/5$  (other values yield equally good agreement). As before, the approximation works well at temperatures up to  $T_c/5$  (and, in this case, perhaps even higher).

## SUMMARY AND CONCLUDING REMARKS

We have constructed explicit, twice-differentiable approximants for the full anisotropy of step stiffness and line tension on both {001} and {111} surfaces of fcc crystals. These expressions are accurate over a broad range of experimentally relevant temperatures; they fail only when the stiffness is nearly isotropic, i.e., when their use is no longer required. Implementation into continuum simulations straightforward and efficient. They are much more usable than numerically extracting solutions from the underlying 6th-order equations, and more flexible and convenient than constructing immense look-up tables as functions of angle and temperature from such a procedure. Our expressions are greatly superior to conventional explicit formulas for step stiffness and line tension, which usually take the form of simple sinusoidal variation that neither carry temperature dependence nor accurately capture the anisotropy (extreme for the step stiffness) observed at lower temperatures. For clarity and convenience, we summarize our results in Table I.

We have implemented these formulas into state-of-the-art finite-element simulations and are currently using them to compare with recent experiments monitoring the relaxation of depinned steps on Ag(111) [18].

### Acknowledgements

This work was supported primarily by the MRSEC at the University of Maryland under NSF Grant DMR 05-20471, with partial support from DOE CMSN grant DEFG0205ER46227. Seminal discussions took place at the Fall 2005 UCLA/IPAM program “Bridging Time and Length Scales in Materials Science and Bio-Physics.” We thank D. Margetis and A. Voigt for helpful discussions.

---

\* tjs@glue.umd.edu

† einstein@umd.edu; <http://www2.physics.umd.edu/~einstein/>

- [1] Axel Voigt, Ed. *Multiscale Modeling in Epitaxial Growth*, International Series of Numerical Mathematics Vol. 149, Birkhäuser, Basel (2005).
- [2] M. Schimschak and J. Krug, *Surface electromigration as a moving boundary value problem*, Phys. Rev. Lett. 78 (1997) 278–281; *Electromigration-induced breakup of two-dimensional voids*, Phys. Rev. Lett. 80 (1998) 1674–1677.
- [3] O. Pierre-Louis and T. L. Einstein, *Electromigration of single-layer clusters*, Phys. Rev. B 62 (2000) 13697–13708.
- [4] E.g., K Thürmer, D.-J. Liu, E. D. Williams, and J. D. Weeks, *Onset of step antibanding instability due to surface electromigration*, Phys. Rev. Lett. 83 (1999) 5531–5534 .
- [5] M. Ondrejcek, W. Swiech, C. S. Durfee, and C. P. Flynn, *Step fluctuations and step interactions on Mo(011)* Surface Sci. 541 (2003) 31–45.
- [6] N. C. Bartelt, T. L. Einstein, and E. D. Williams, *The influence of step step interactions on step wandering*, Surface Sci. 240 (1990) L591-L598, and references therein.
- [7] H.-C. Jeong and E. D. Williams, *Steps on surfaces: experiment and theory*, Surface Sci. Rept. 34 (1999) 171–294.
- [8] E. Bänsch, F. Hausser, O. Lakkis, B. Li, and A. Voigt, *Finite element method for epitaxial growth with attachement-detachment kinetics*, J. Comput. Phys. 194 (2004) 409–434.
- [9] E. Bänsch, F. Hausser, and A. Voigt, *Finite element method for epitaxial growth with thermodynamic boundary conditions*, SIAM J. Sci. Comput. 26 (2005) 2029–2046.
- [10] L. Balykov and A. Voigt, *A 2 + 1 dimensional terrace-step-kink model for epitaxial growth far from equilibrium*, Multiscale Model. Simul. 5 (2006) 45–61.
- [11] T. J. Stasevich, T. L. Einstein, R. K. P. Zia, M. Giesen, H. Ibach, and F. Szalma, *Effects of next-nearest-neighbor interactions on the orientation dependence of step stiffness: Reconciling theory with experiment for Cu(001)*, Phys. Rev. B 70 (2004) 245404/1–7.
- [12] T. J. Stasevich, H. Gebremariam, T. L. Einstein, M. Giesen, C. Steimer, and H. Ibach, *Low-temperature orientation dependence of step stiffness on 111 surfaces*, Phys. Rev. B 71 (2005) 245414/1–10.
- [13] V. B. Shenoy and C. V. Ciobanu, *Orientation dependence of the stiffness of surface steps: an analysis based on anisotropic elasticity*, Surface Sci. 554 (2004) 222–232.
- [14] R. K. P. Zia, *Exact equilibrium shapes of Ising crystals on triangular/honeycomb lattices*, J. Stat. Phys. 45 (1986) 801–813.
- [15] J. D. Faires and R. Burden, *Numerical Methods*, 2nd ed., Brooks/Cole Publishing Co. Pacific Grove, CA, 1998.
- [16] D. B. Abraham and P. Reed, *Diagonal interface in the two-dimensional Ising ferromagnet*, J. Phys. A 10 (1977) L121–123.
- [17] N. Akutsu and Y. Akutsu, *Step stiffness and equilibrium island shape of Si(100) surface: statistical-mechanical calculation by the imaginary path weight random-walk method*, Surf. Sci. 376 (1997) 92–98.
- [18] T. J. Stasevich, C. Tao, F. Hausser, A. Voigt, E. D. Williams, and T. L. Einstein, unpublished.